

Chapter 10 Sensitivity analysis of ethanol production process using Aspen Plus

Capítulo 10 Análisis de sensibilidad del proceso de producción de etanol utilizando Aspen Plus

SÁNCHEZ-OROZCO, Raymundo†*, BERNAL-MARTÍNEZ, Lina Agustina and SALAZAR-PERALTA Araceli

Tecnológico de Estudios Superiores de Jocotitlán, Carretera Toluca-Atacomulco Km 44.8, Ejido de San Juan y San Agustín, C.P. 50700, Jocotitlán, México

ID 1st Author: *Raymundo, Sánchez-Orozco* / **ORC ID:** 0000-0003-0006-1711, **CVU CONACYT ID:** 169684

ID 1st Co-author: *Lina-Agustina, Bernal-Martínez* / **ORC ID:** 0000-0002-4922-043X, **CVU CONACYT ID:** 173701

ID 2nd Co-author: *Araceli, Salazar-Peralta* / **ORC ID:** 0000-0001-5861-3748, **CVU CONACYT ID:** 300357

DOI: 10.35429/H.2022.3.144.160

R. Sánchez, L. Bernal, and A. Salazar

*r.sanchez@tesjo.edu.mx

A. Ledesma (AA.). Science of Technology and Innovation. Handbooks-TII-©ECORFAN-Mexico, 2022.

Abstract

In this work, a sustainable process for the production of ethanol from the monosaccharide glucose was simulated. The thermodynamic model used for the process was NRTL-RK (based on activity coefficients) due to the polar nature and non-ideal behavior of the species involved. The process was carried out in three steps. First, glucose in aqueous solution was subjected to a fermentation process using a stoichiometric reactor. The second stage consisted of carbon dioxide degassing using two flash tank systems. In the third stage, a RadFrac distillation column was used to facilitate the separation of ethanol and water. According to the results obtained, the molar flow rate of the distilled product stream was 5.04 kmol/h with a composition of 82.15% mol of ethanol, 15.37% mol of water and 2.47% mol of carbon dioxide, while the bottom stream whose molar flow rate was 143.39 kmol/h had a composition of 99.99% mol of water with traces of ethanol and carbon dioxide. The results obtained demonstrate that ethanol production from glucose is possible.

Bioethanol, Simulation, Sustainable

Resumen

En este trabajo, se simuló un proceso sostenible para la producción de etanol a partir del monosacárido glucosa. El modelo termodinámico utilizado para el proceso fue NRTL-RK (basado en coeficientes de actividad) debido a la naturaleza polar y al comportamiento no ideal de las especies involucradas. El proceso se llevó a cabo en tres etapas. En primer lugar, la glucosa en solución acuosa se sometió a un proceso de fermentación utilizando un reactor estequiométrico. La segunda etapa consistió en la desgasificación de dióxido de carbono utilizando dos sistemas de tanques flash. En la tercera etapa, se utilizó una columna de destilación RadFrac para facilitar la separación de etanol y agua. De acuerdo con los resultados obtenidos, el caudal molar de la corriente de producto destilado fue de 5.04 kmol/h con una composición de 82.15% mol de etanol, 15.37% mol de agua y 2.47% mol de dióxido de carbono, mientras que la corriente inferior cuyo caudal molar fue de 143.39 kmol/h tuvo una composición de 99.99% mol de agua con trazas de etanol y dióxido de carbono. Los resultados obtenidos demuestran que la producción de etanol a partir de glucosa es posible.

Bioetanol, Simulación, Sustentable

1. Introduction

Chemical compounds of renewable origin are coming to the forefront with the purpose of reducing pressure on oil reserves and above all, due to the lower environmental impacts caused compared to their fossil counterparts (Alio et al., 2019; Cardona et al., 2018; Kim et al., 2017). This trend is occurring as a result of several factors influencing human life and the economy worldwide: climate change, unstable oil prices, the search for alternative chemical sources, and the vision of ensuring security of energy supply due to ever-increasing global demand. However, stand-alone bioprocesses can present high operational costs, which can be reduced by process integration with a consolidated facility (Olofsson et al., 2017; Zhou et al., 2018; Sharma et al., 2020). In order to meet these supply needs while providing an economically viable option, the concept of biorefinery production was created (Abdou et al., 2020; Battista et al., 2019; Gil et al., 2014; Li et al., 2016; Morales et al., 2017; Morales et al., 2021).

In biorefineries, a number of different processes are used to fractionate biomass into various products, as in petroleum refineries, but working with a different and renewable feedstock. The purpose is also very similar to that of a petroleum refinery: to produce compounds for both the chemical industry and the fuel market (Tan et al., 2020; Zabed et al., 2016; Singh et al., 2017; Rodrigues et al., 2018; Kumar and Singh, 2016). Bioethanol, the most widespread chemical and fuel derived from renewable sources, has a consolidated market in the world and a large share in the Brazilian fuel market.

Bioethanol is one of the most promising alternative fuels to reduce fossil fuel consumption in the transportation sector (Kim et al., 2016; Isikgor and Becer, 2015; Chrysikou et al., 2018; Chandel et al., 2018). The economic viability of the bioethanol industry depends on a sufficient supply of high-quality, low-cost, bio-based renewable feedstocks and efficient biomass-to-bioethanol conversion technologies.

Consequently, biofuels, especially of the second generation, have gained great interest in the view of current environmental problems and oil dependence (Chin et al., 2020; Borand and Karaosmanoglu, 2018; Ardila et al., 2014; Bahry et al., 2017). Bioethanol used for commercial purposes is generally produced from edible feedstocks such as corn and sugarcane, which increases the cost of production. The high cost of these feedstocks is the driving force behind the search for second and third generation bioethanol produced from cheaper and more readily available feedstocks.

When bioethanol is produced from edible feedstocks such as corn and sugarcane, it is called first generation (1G) bioethanol and second generation (2G) 2G bioethanol if the feedstock is lignocellulose (Ashraf and Schmidt, 2018; Brown, 2015; Choi et al., 2019; Daylan and Ciliz, 2016). Examples of lignocellulosic biomass include corn stalks, wood, herbaceous crops, waste paper and paper products, agricultural and forestry residues, pulp and paper mill waste, municipal solid waste, and food industry waste. Lignocellulosic biomass consists of cellulose, hemicellulose, lignin, protein, ash and minor extractives (Hoang et al., 2020; Gnansounou and Dauriat, 2010; Vieira et al., 2020; Sarks et al., 2014; García-Velásquez et al., 2019). Lignocellulosic sources are the most promising feedstocks, have the highest potential and constitute an important part of most future emissions scenarios consistent with stringent climate change mitigation targets (Romaní et al., 2019; Tan et al., 2016; Zabed et al., 2017; Zhang et al., 2016; Devarapalli et al., 2017). Lignocellulosic feedstocks include woody (softwood and hardwood) and herbaceous (perennial grasses) energy crops, agricultural residues (cereal straw, stubble and bagasse), forest residues (sawdust, pruning and bark residues) and organic portions of municipal solid waste (Abdou et al., 2020; Cardona et al., 2018; Gil et al., 2014). Bioethanol production from lignocellulosic biomass materials typically has lower life-cycle greenhouse gas (GHG) emissions and lower risks to compete with food security than bioethanol production from food crops (Li et al., 2016; García-Velásquez et al., 2019).

Lignocellulosic biomass is being considered as a feedstock for bioethanol production due to the relatively low cost of acquisition, availability and sustainability of supply. 2G bioethanol has a greater potential to reduce greenhouse gas emissions compared to 1G bioethanol. Third generation (3G) bioethanol is obtained when algae are used as feedstock (Morales et al., 2021; Oliva et al., 2020). Algae bioethanol is possibly gaining ground due to the high carbohydrate content and the absence of lignin in most of the available algae. Despite efforts to reduce the cost of production by using various non-edible materials, the cost of processing the feedstock is still very high, making bioethanol uncompetitive with conventional gasoline (Romaní et al., 2019; Zhou et al., 2018). Life cycle assessment and techno-economic analyses are generally performed to evaluate the economic feasibility and environmental impact of bioethanol production processes (Cardona et al., 2018; Ardila et al., 2014; Hoang et al., 2020).

The chemical industry has long employed simulation strategies to design and optimize process operations. Initially simple models of unit operations (using multiple assumptions and simplifications to facilitate calculations) that could be solved by hand or mechanical calculators were employed, and later evolved to more sophisticated and rigorous models that can only be solved by computers (Nosrati-Ghods et al., 2020; Gil et al., 2014). The importance of computers in this context is that simplifying assumptions are no longer needed to facilitate computations. In addition, computers solve the operations of process units, so connecting several process streams (complete with recycles) and having the computer repeat the calculations until the matter and energy balances are balanced is relatively easy. Thus sequential modular process simulation for complete flowsheets was born (Gabhane and Kapoor, 2019).

Currently, the integration of simulation tools in process development is often used to analyze economic feasibility, performance, optimization and parameter estimation; therefore, it facilitates equipment design, sizing and cost evaluation (Daylan and Ciliz, 2016). Chemical process simulation provides unbiased material/energy data of production processes with reduced time and resource utilization for data collection (Gil et al., 2014). Simulations have the flexibility of effective process data predictions based on appropriate thermodynamic properties, design parameters, and actual plant conditions for individual plant designs. In addition, pre-production/modification process plants can be easily predicted using simulations to integrate/modify different alternative scenarios (Gabhane and Kapoor, 2019). For example, additions of new materials, technologies and recycling options in different processes can be easily realized, to evaluate their benefits and plan decisions for the industry (Chandel et al., 2018).

Several studies have been conducted to obtain ethanol from sugarcane juice (Vieira et al., 2020). It has also been reported that the use of this raw material represents 40% of the total cost of ethanol production and that this cost decreases when using sugarcane bagasse. However, the main limitation is the high degree of complexity associated with its processing and even more with its simulation.

In this work, the production of ethanol from glucose was simulated using Aspen Plus® version 11. The NRTL-RK thermodynamic model was used. The process was carried out in three stages, first, a fermentation process using a stoichiometric reactor. The second stage consisted of carbon dioxide degassing through flash tanks and finally, in the third stage, distillation in a RadFrac column to promote the separation of ethanol and water.

2. Methodology

2.1 General description of the process

For the design and simulation of the ethanol production process, a fermenter (FERM) was fed sugar (GLUCOSE in aqueous solution) along with yeast to produce ethanol and CO₂ as a by-product. The fermenter product was processed in two degassing stages (DEGAS1 and DEGAS2) to remove most of the CO₂ produced. The liquid product was fed to a RadFrac distillation column (COL1) to remove water and concentrate the ethanol. In the fermentation section for the transformation of glucose to ethanol, an aqueous glucose solution was fed to a fermenter along with an additional water stream to control the concentration. The fermenter product was degassed in a single-stage separator to remove most of the CO₂ produced by the fermentation process. The liquid product from the separator was pumped to a heater where it exchanged heat with the bottoms of the ethanol column prior to being fed to a second degassing tank. Additional CO₂ was removed in the second separator and the resulting liquid product was fed to the ethanol distillation column. The ethanol column removed most of the water in the bottom stream, concentrating the ethanol in the distillate. The distillation column, equipped with 38 stages, a reboiler and a total condenser, operated at a pressure of 50 psig. The distillate-to-feed column ratio specification was adjusted to maintain the ethanol purity specification in the column bottoms product. The specifications needed to construct the flowsheet are provided in Tables 1.1, Table 1.2 and Table 1.3.

Table 1.1 Component data and method of ownership

	ID	Type	Formula	Name
List of components	ETOH	CONV	C2H2O-2	ETHANOL
	WATER	CONV	H2O	WATER
	GLUCOSE	CONV	C6H12O6	DEXTROSE
	CO ₂	CONV	CO2	CARBON DIOXIDE
Method of ownership	NRTL-RK			
Henry's components	CO ₂			
Binary data	NRTL and Henry's binary forms			

Source: Own Elaboration

Table 1.2 Parameters of the feed streams

Parameter	Units	FERMFEED	H2OFEED
Mass flow			
GLUCOSE	kg/h	380	
WATER	kg/h	1150	
Temperature	°C	27	
Pressure	bar	2.5	
Mass fraction			
WATER			1
Temperature	°C		27
Pressure	bar		2.5
Mass flow	kg/h		1450

Source: Own Elaboration

Table 1.3 Operating conditions of the process equipment

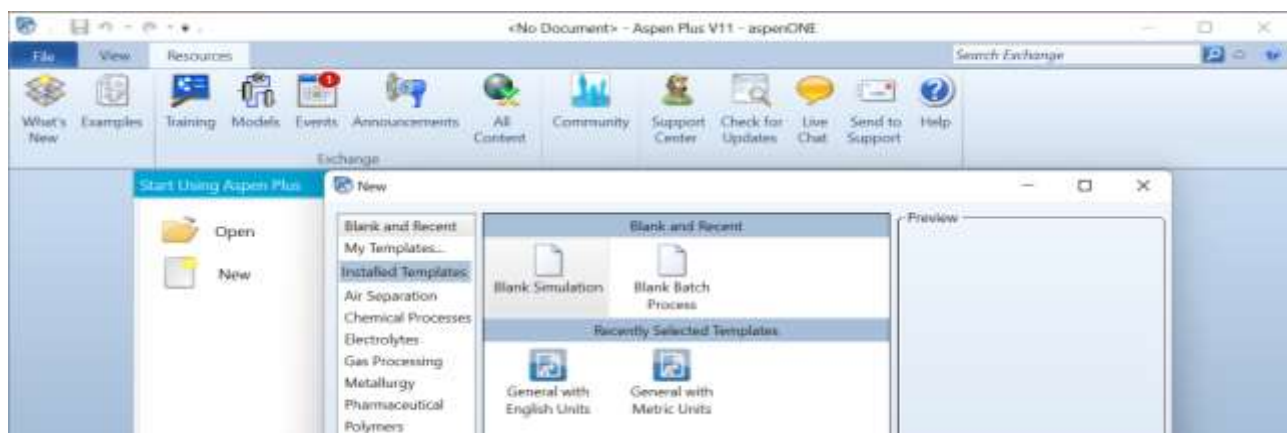
Process equipment	Units	Parameter and/or value
FERM		
Temperature	°C	32
Pressure drop	bar	0
Reaction		GLUCOSE → 2ETHANOL + 2CO ₂
Reaction conversion		1.0, key component: GLUCOSE
DEGAS1		
Pressure drop	bar	0
Heat requirement	cal/h	0
PUMP		
Increased pressure	bar	7
PREHEAT		
Calculation method		Short
Difference hot outlet-cold inlet	°F	10
DEGAS2		
Pressure drop	bar	0
Heat requirements	cal/h	0
COL1		
Number of stages		40 (including condenser and reboiler)
Condenser type		Total
Type of reboiler		Kettle
Convergence method		strongly non-ideal liquid
Reflux ratio		30
Distillate-to-food ratio		0.034
Column feed stage		30 (top stage)
Top stage pressure	bar	5

Source: Own Elaboration

2.2 Process modeling with Aspen Plus

To start the program and to perform a new simulation, it was necessary to select the New option in Figure 1.1, belonging to the Aspen Plus V11 program of the aspenONE® package, then click on Blank Simulation and then on Create.

Figure 1.1 Aspen Plus V11 home page



Source: Own Elaboration

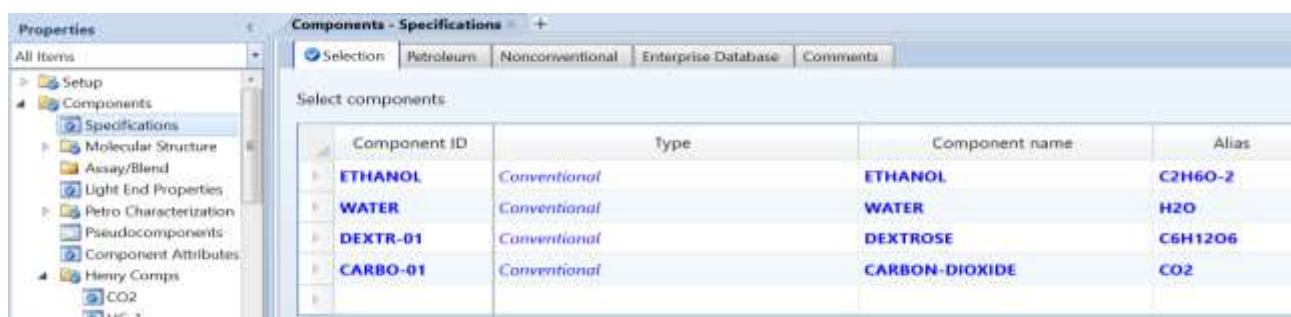
2.3 Specification of chemical components

The first step in preparing the process simulation was to establish the chemical basis for the model. This consisted of choosing the components to be included in the material balance and deciding which model to use for the prediction of physical properties and phase equilibrium. The program has an extensive list of components with their properties, and it was sufficient to select them (Figure 1.2). The components were chosen by double-clicking on them, or by highlighting the component and clicking on Add selected compounds. The name of each compound could also be typed directly into the corresponding boxes. Once all the compounds were selected, the thermodynamic model was defined.

2.4 Selection of the thermodynamic model

Once the components were specified, the thermodynamic model was chosen. This model was used to calculate the thermodynamic and transport properties of the components and their mixtures, such as enthalpy, entropy, density, specific heat, L-V equilibrium, etc. Therefore, the correct selection of the model was very important (Figure 1.3). In general, properties were calculated with equations of state (EOS), activity coefficient models (γ models) and special models (theoretical, empirical or hybrid correlations). The EOS models represented the liquid and vapor phases, while the gamma models represented only the liquid phase of the system. For this reason, they are used in conjunction with an equation of state to represent the vapor. Once the property specifications were completed, the property prediction by the proposed model was analyzed to ensure correct results. This was done using the Property Analysis function of Aspen Plus. The property analysis generated tables of physical property values, which were used to better visualize and understand the behavior of the properties as predicted by the property specifications.

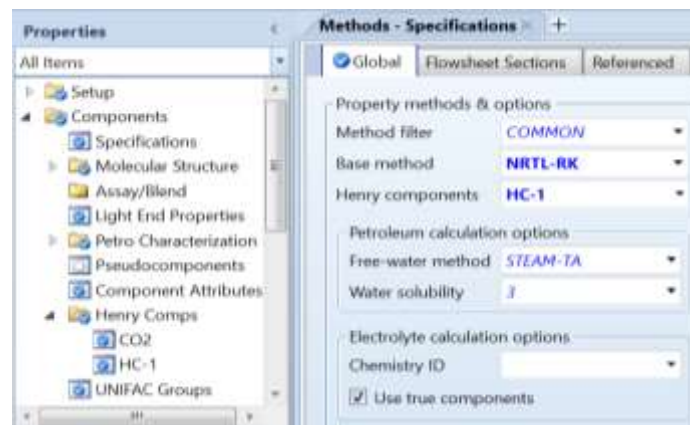
Figure 1.2 Component specification from the database



Component ID	Type	Component name	Alias
ETHANOL	Conventional	ETHANOL	C2H6O-2
WATER	Conventional	WATER	H2O
DEXTR-01	Conventional	DEXTROSE	C6H12O6
CARBO-01	Conventional	CARBON-DIOXIDE	CO2

Source: Own Elaboration

Figure 1.3 Specifications of the method for identifying thermodynamic properties

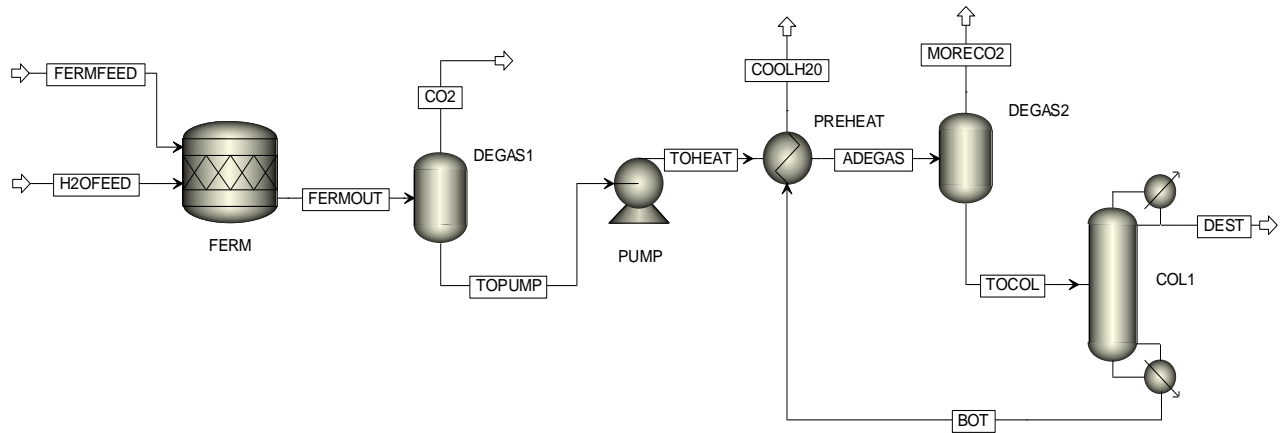


Source: Own Elaboration

2.5 Process flow diagram in Aspen Plus

The stages involved in ethanol production from dextrose included fermentation, gasification, syngas purging and methanol synthesis. The model was built using a general template with units in the metric system, adding the components and selecting the NRTL thermodynamic method (based on activity coefficients) in combination with the Redlich-Wong equation of state (NRTL-RK), and then performing the flow diagram in Aspen Plus as shown in Figure 1.4. Finally, the operating conditions of each process equipment were specified and the simulation was run. When the simulation converged it was possible to access the results through the toolbar in the Stream Summary option.

Figure 1.4 Process flow diagram for ethanol synthesis in Aspen Plus



Source: Own Elaboration

3. Results

3.1. Behavior of the ethanol-water system

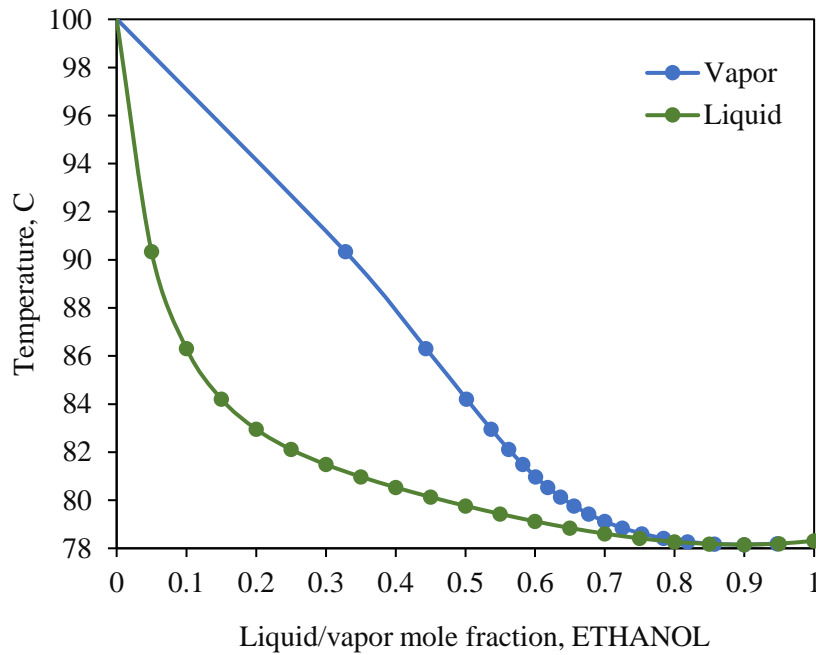
The vapor liquid equilibrium (VLE) curve of the ethanol-water system is shown in Figure 1.5. It can be seen that atmospheric distillation of this mixture is possible only to a certain extent. The maximum purity that can be achieved by atmospheric distillation is 95% by weight, because as soon as the composition reached 95.6% by weight (4.4% by weight of water) the azeotrope was formed. The mixture of ethanol and water forms a positive azeotrope. Ethanol boils at 78.4 °C and water at 100 °C. However, the boiling point of the azeotrope was 78.2 °C, which is lower than its two components.

Generally a positive azeotrope bubbles at a lower temperature than some other proportion of its constituents. For the binary ethanol/water system, 78.2 °C was the base temperature for the mixture to bubble at atmospheric pressure. Positive azeotropes are also known as lower boiling mixtures or minimum boiling azeotropes (Gil et al., 2014). Figure 1.6 shows the x-y plot of liquid equilibrium data generated by regression with the binary interaction parameters of the NRTL-RK thermodynamic model.

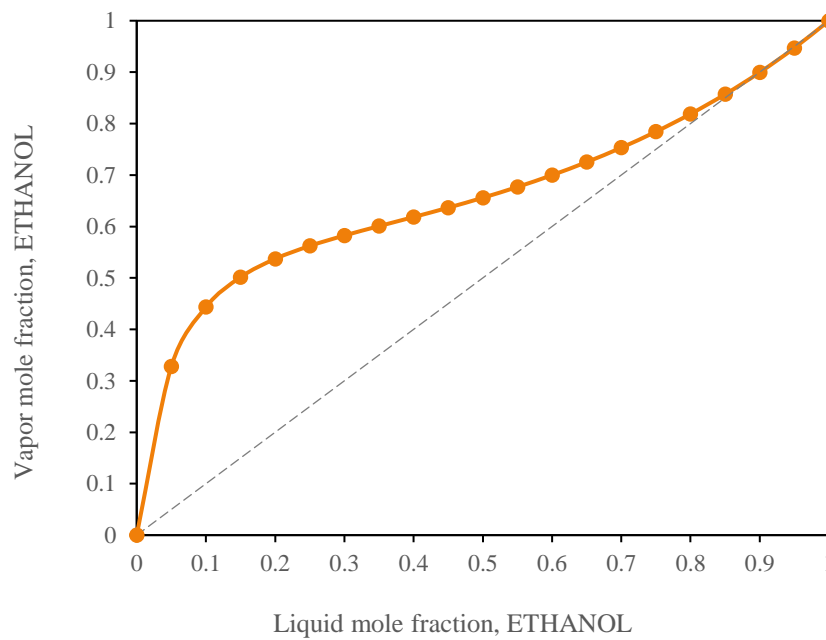
3.2 Composition profiles and molar flows

Figure 1.7 shows the profile of ethanol and water compositions through the distillation column. It can be observed that in stage 1 (condenser) the maximum concentration of ethanol and a small percentage of water was reached due to the azeotropic behavior of the mixture, likewise, it is notable that in stage 40 (boiler) it is almost entirely made up of water, there is only a small fraction of ethanol that was not recovered by the concentrator column. In addition, the liquid phase composition profile showed that the ethanol concentration decreased from stage 30 due to the feed stream.

Thus, also, the observed change in ethanol composition was due to the presence of an azeotrope in the mixture. The ethanol composition increased in the upper stages of the column, while the water composition was concentrated in the bottom stream of the column.

Figure 1.5 T-x-y diagram for ETHANOL/WATER

Source: Own Elaboration

Figure 1.6. x-y diagram for ETHANOL/WATER

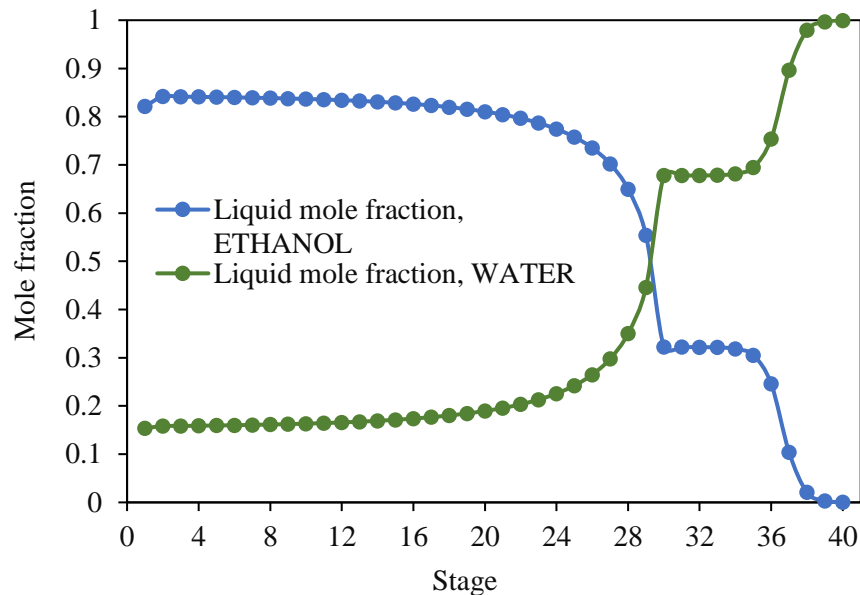
Source: Own Elaboration

The molar flow profiles of the vapor and liquid phases as a function of the number of stages in the distillation column are shown in Figure 1.8. It can be seen that the dilute ethanol feed is introduced starting at stage 30 where it comes in contact with the vapor which is at very high temperature and immediately begins to change phase. It then moves to the condenser where the steam is extracted as condensate and the ethanol mixture as distillate. The significant change in the liquid molar flux is primarily attributed to the feed stream of the azeotropic mixture.

This change was caused by the liquid phase vaporization due to the inlet temperature of water. Meanwhile, the vapor phase molar flux remained constant throughout the column. Moreover, as the distillation progressed, the composition of the distillate became richer in the less volatile component (ethanol), therefore the composition richest in ethanol corresponded to the first drop of distillate obtained. At this point it was also possible to analyze the distillation yield, i.e., when a greater mass of distillate was obtained, the ethanol composition tended to decrease.

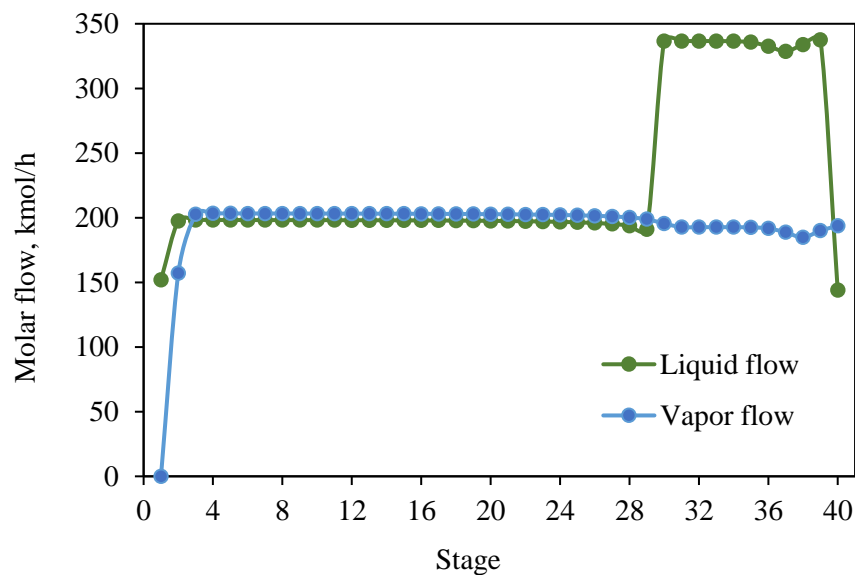
In some processes a purer distillate is required, which is in contrast to the amount that can be obtained. In general, the longer the column and the larger the contact surface within the column, the more effective the separation of the components will be, although it also depends on other factors (Abdou et al., 2020).

Figure 1.7. Profile of compositions in the distillation column for ETHANOL/WATER



Source: Own Elaboration

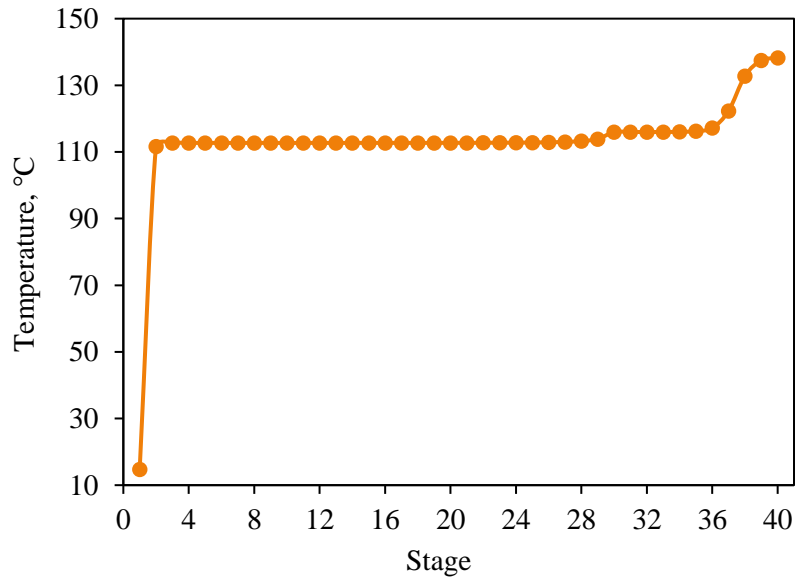
Figure 1.8 Vapor-liquid molar flow profile in the distillation column



Source: Own Elaboration

3.3 Temperature profiles through the distillation column

The behavior of the temperature profile in the column showed changes starting at stage 30 due to the feed stream of the azeotropic mixture. A significant increase in temperature was observed from stages 36 to 40 due to the proximity to the kettle (Figure 1.9). The temperature profile is of great help in controlling the purity of the column products since generally the composition is usually complicated and time consuming to measure, whereas the temperature offered a quick and simple measurement that being related to the composition at each stage of the column facilitates column control.

Figure 1.9 Temperature profile in the distillation column for ETHANOL/WATER

Source: Own Elaboration

3.4 Composition and conditions in process streams

After the simulation, process data such as mass flow, mole fractions of the components, final thermodynamic data, as well as the feed and outlet conditions of the reactor, flash separation tank and distiller were determined. Table 1.4 and Table 1.5 summarize the results according to each process equipment and stream involved. It is observed that the conversion of glucose is total and that the flow at the outlet of the stoichiometric reactor is constituted by 194.34 kg/hr of ethanol, 2600 kg/hr of water and 185.65 kg/hr of carbon dioxide. After this stream passes through the first flash separator, the mass flow of the outlet stream contains 173.09 kg/hr of carbon dioxide, 0.69 kg/hr of ethanol and 0.93 kg/hr of water. Since the gas generated in the fermentation process was not completely eliminated, it was necessary to place a second flash separator to separate the remaining carbon dioxide, which is equivalent to 7.06 kg/h. Subsequently, the mixture of ethanol and water was sent to a distillation column, where it separated the ethanol in the distillate stream and the water in the bottoms stream.

Table 1.4 Overall results of the process simulation (Part 1)

		FERMFEED	H2OFEED	FERMOUT	CO ₂	TOHEAT
Phase		Liquid	Liquid	Liquid	Vapor	Liquid
Temperature	C	27	27	32	25.3547	25.8016
Pressure	bar	2.5	2.5	2.5	2.5	9.5
Mole frac vapor		0	0	0	1	0
Mole frac liquid		1	1	1	0	1
Molar Enthalpy	cal/mol	-75782.6505	-68226.4504	-68934.8065	-93393.2488	-68266.2224
Mass Enthalpy	cal/gm	-3266.2800	-3787.1435	-3533.6950	-2138.0999	-3620.0425
Molar Entropy	cal/mol-K	-46.1415	-38.8489	-39.1185	-1.3066	-40.0025
Mass Entropy	cal/gm-K	-1.9887	-2.1564	-2.0053	-0.0299	-2.1213
Molar density	mol/cc	0.0472	0.0551	0.0504	0.0001	0.0519
Mass density	gm/cc	1.0954	0.9920	0.9833	0.0045	0.9783
Average PM		23.2015	18.0153	19.5079	43.6805	18.8579
Molar flows	kmol/hr	65.9440	80.4872	152.7590	4.0001	148.7589
ETHANOL	kmol/hr	0.0000	0.0000	4.2185	0.0151	4.2034
WATER	kmol/hr	63.8347	80.4872	144.3219	0.0519	144.2701
DEXTR-01	kmol/hr	2.1093	0	0	0	0
CARBO-01	kmol/hr	0	0	4.2185	3.9331	0.2854
Mole fractions						
ETHANOL		0	0	0.0276	0.0038	0.0283
WATER		0.9680	1	0.9448	0.0130	0.9698
DEXTR-01		0.0320	0	0	0	0
CARBO-01		0	0	0.0276	0.9832	0.0019
Mass flows	kg/hr	1530	1450	2980.0000	174.7278	2805.2722
ETHANOL	kg/hr	0	0	194.3435	0.6977	193.6457

WATER	kg/hr	1150	1450	2600	0.9345	2599.0655
DEXTR-01	kg/hr	380	0	0	0	0
CARBO-01	kg/hr	0	0	185.6565	173.0955	12.5611
Mass fractions						
ETHANOL		0	0	0.0652	0.0040	0.0690
WATER		0.7516	1	0.8725	0.0053	0.9265
DEXTR-01		0.2484	0	0	0	0
CARBO-01		0	0	0.0623	0.9907	0.0045
Volumetric flow	L/min	23.2802	24.3609	50.5076	653.5067	47.7908

Source: Own Elaboration

Table 1.5 Overall results of the process simulation (Part 2)

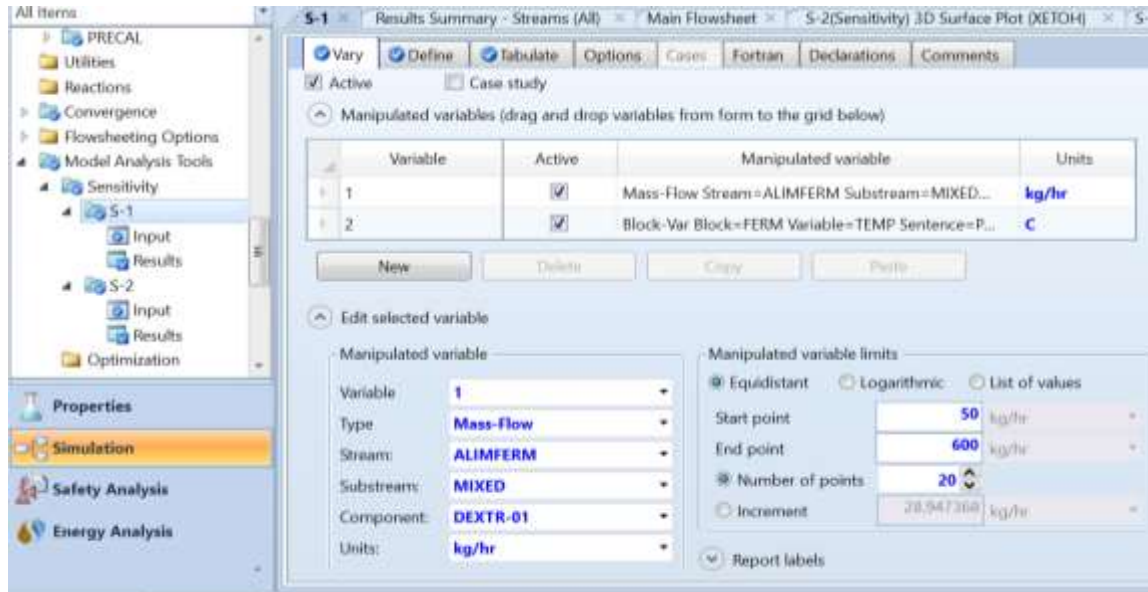
		COOLH2O	MORECO2	TOCOL	DEST	BOT
Phase		Liquid	Vapor	Liquid	Liquid	Liquid
Temperature	C	31.3572	139.4568	139.4568	40.2237	151.8516
Pressure	bar	5	9.5	9.5	5	5
Mole frac vapor		0	1	0	0	0
Mole frac liquid		1	0	1	1	1
Mole frac vapor		0	1	0	0	0
Molar Enthalpy	cal/mol	-68147.9486	-74985.7582	-66037.4053	-66943.8275	-65855.4427
Mass Enthalpy	cal/gm	-3781.9021	-2177.4567	-3508.0010	-1605.1766	-3654.6784
Molar Entropy	cal/mol-K	-38.5986	-9.2021	-33.8624	-72.3739	-32.3353
Mass Entropy	cal/gm-K	-2.1420	-0.2672	-1.7988	-1.7354	-1.7945
Molar density	mol/cc	0.0548	0.0003	0.0455	0.0191	0.0478
Mass density	gm/cc	0.9877	0.0099	0.8564	0.7962	0.8609
Average PM		18.0195	34.4373	18.8248	41.7050	18.0195
Molar flows	kmol/h	143.3968	0.3149	148.4439	5.0471	143.3968
ETHANOL	kmol/h	0.0215	0.0356	4.1677	4.1462	0.0215
WATER	kmol/h	143.3753	0.1188	144.1513	0.7760	143.3753
DEXTR-01	kmol/h	0	0	0	0	0
CARBO-01	kmol/h	0	0.1605	0.1249	0.1249	0.0000
Mole fractions						
ETHANOL		0.0002	0.1132	0.0281	0.8215	0.0002
WATER		0.9998	0.3772	0.9711	0.1537	0.9998
DEXTR-01		0	0	0	0	0
CARBO-01		0	0.5096	0.0008	0.0248	0.0000
Mass flows	kg/h	2583.9375	10.8459	2794.4264	210.4888	2583.9375
ETHANOL	kg/h	0.9915	1.6422	192.0036	191.0120	0.9915
WATER	kg/h	2582.9460	2.1403	2596.9252	13.9792	2582.9460
DEXTR-01	kg/h	0	0	0	0	0
CARBO-01	kg/h	0	7.0635	5.4976	5.4976	0
Mass fractions						
ETHANOL		0.0004	0.1514	0.0687	0.9075	0.0004
WATER		0.9996	0.1973	0.9293	0.0664	0.9996
DEXTR-01		0	0	0	0	0
CARBO-01		0	0.6513	0.0020	0.0261	0
Volumetric flow	l/min	43.6013	18.2609	54.3808	4.4063	50.0216

Source: Own Elaboration

3.5 Sensitivity analysis

One of the advantages of the simulation of the proposed system was that the performance sensitivity of the process to changes in the operating variables could be studied. With Aspen, the inputs were manipulated, and the effect was tabulated in a set of results according to the chosen variables. In general, the sensitivity analysis was performed to evaluate the parametric conditions of the process. The initial value for molar flux (glucose in aqueous solution) in the stoichiometric reactor was selected based on literature review (Cardona et al., 201; Gil et al., 2014) and subsequently investigated with sensitivity analysis (Figure 1.10).

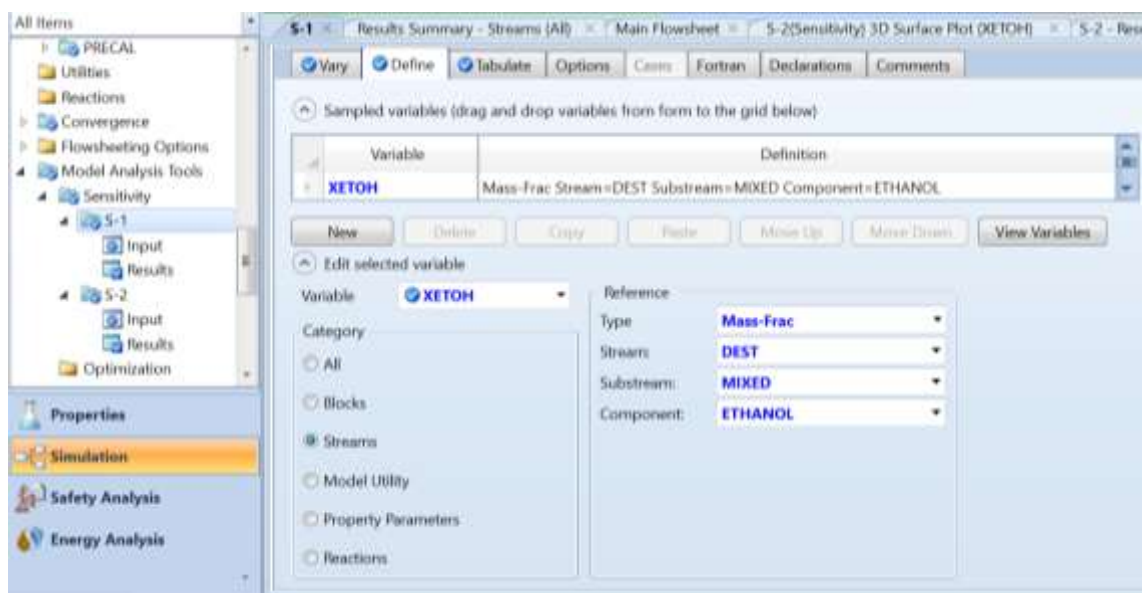
Figure 1.10 Sensitivity analysis of the manipulated variable



Source: Own Elaboration

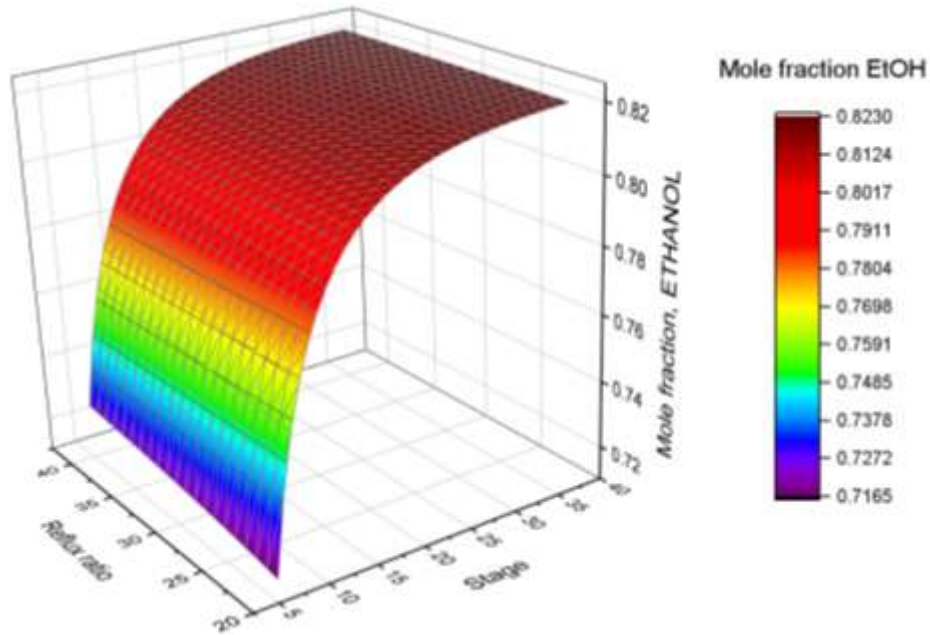
The influence of the molar flow rate in the reactor feed stream, the number of theoretical stages, as well as the reflux ratio required in the distillation column was analyzed with the purpose of maximizing ethanol production and making the process as cost-effective as possible. The sensitivity analysis was performed in the range of 50 to 600 kg/h of glucose in the reactor feed stream, while the reflux ratio was evaluated in the range of 20 to 40. For this analysis, the non-manipulable variable was the ethanol mass fraction in the upper stream of the distillation column (distillate) as shown in Figure 1.11. Thus, the process performance was evaluated through the manipulation of three independent variables (feed flow, column reflux ratio and number of caps) and one dependent variable (ethanol mass fraction). To analyze the influence of variables such as reflux ratio and feed stage on the distillation column, sensitivity analyses were developed using a surface plot (Figure 1.12). Through this tool, the reflux ratio values were varied from 20 to 40 and the feed stage from 5 to 40 to evaluate how the composition of anhydrous ethanol in the distillate stream changed. It is observed that as the feed stage approaches the kettle, the mole fraction of anhydrous ethanol increases, indicating that higher stages promote greater vaporization of the liquid fraction. This represents a benefit for the process because the objective is to obtain the highest possible purity in the separation of anhydrous ethanol. Regarding the reflux ratio, it was observed that it does not have a significant influence on the ethanol composition, i.e. an increase from 20 to 40 did not promote greater purity in the distillate composition.

Figure 1.11 Definition of parameters for sensitivity analysis as a function of the ethanol composition in the distilled product



Source: Own Elaboration

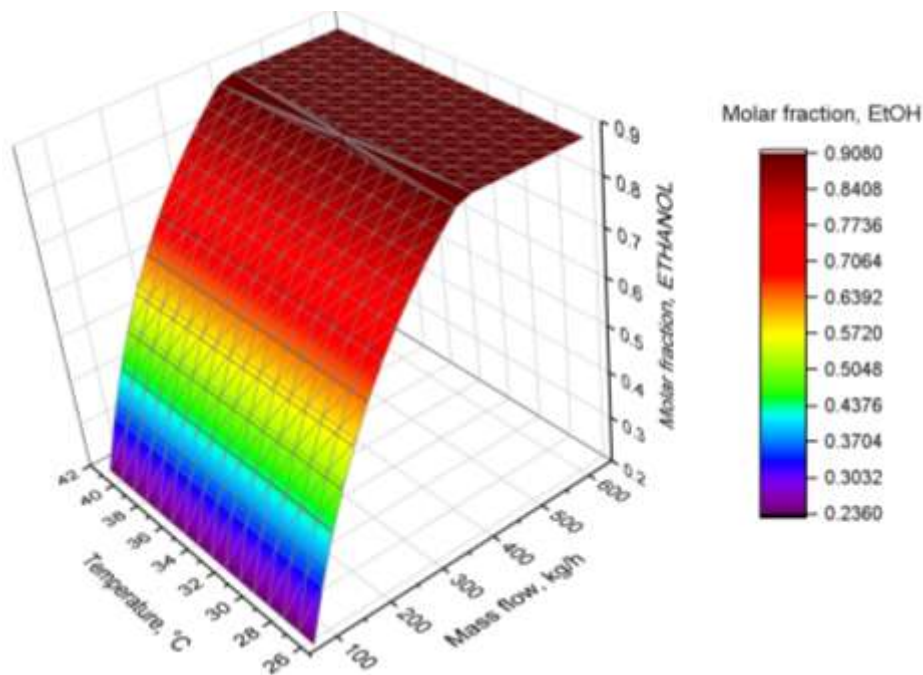
Figure 1.12 Influence of reflux ratio and number of stages on ETHANOL composition



Source: Own Elaboration

Additionally, the dependence of the ethanol mole fraction on the temperature and mass flow rate of the reactor feed stream was evaluated. Figure 1.13 shows that the temperature of the feed stream in the range of 25 to 40 °C has no effect on the ethanol mole composition. Therefore, operating the process with a temperature of 25 °C would be sufficient to achieve a maximum purity of 90% molar ethanol. Likewise, the mass flow of the feed stream evaluated in the range of 50 to 600 kg/h showed that a flow rate of 400 kg/h is sufficient to achieve maximum ethanol purity because at higher flow rates, the molar composition remains constant.

Figure 1.13 Temperature profile in the distillation column for ETHANOL/WATER



Source: Own Elaboration

4. Acknowledgment

The authors would like to thank the Technology of Superior Studies of Jocotitlán for the their kind supports provided for the realization of this research.

5. Conclusions

After evaluating the proposed process in Aspen Plus, we proceeded to the simulation of ethanol production from a stream of 380 kg/h of glucose and 1550 kg/h of water, also knowing that the temperature at which they enter the reactor was 27 °C, reactor temperature of 32 °C without pressure drop, and the distillation column was known to contain 40 plates, a reflux of 30, a flow rate of 148.44 kmol/h, the feed entered through plate 30 and the pressure of plate 1 was 5 bar.

Derived from the above, it was determined that the variables introduced are adequate for the process, this was evidenced by the execution of the simulation, otherwise it would not have achieved convergence. Thus, the distilled product stream with a total molar flow of 5.04 kmol/h had a composition of 82.15% mol of ethanol, 15.37% mol of water and 2.47% mol of carbon dioxide, while the bottoms stream with a total molar flow of 143.39 kmol/h had a composition of 99.99% mol of water with traces of ethanol and carbon dioxide.

Finally, one of the characteristics that stand out in the use of software is that they provide sufficiently reliable data for their application in professional engineering life, on the other hand, although the development of the calculations in an analytical way by an engineer is very good, it is always useful to use computational tools to facilitate the analysis of a process.

References

- Abdou Alio, M., Tugui, O.C., Rusu, L., Pons, A., Vial, C. 2020. Hydrolysis and fermentation steps of a pretreated sawmill mixed feedstock for bioethanol production in a wood biorefinery. *Bioresour. Technol.* 310, 123412. DOI: 10.1016/j.biortech.2020.123412. Retrieved July 4, 2022, from <https://pubmed.ncbi.nlm.nih.gov/32361645/>
- Alio, M.A., Tugui, O.C., Vial, C., Pons, A. 2019. Microwave-assisted Organosolv pretreatment of a sawmill mixed feedstock for bioethanol production in a wood biorefinery. *Bioresour. Technol.* 276, 170–176. DOI: 10.1016/j.biortech.2018.12.078. Retrieved July 4, 2022, from <https://www.sciencedirect.com/science/article/pii/S0960852418317498>
- Ardila, Y., Efren, J., Figueroa, J., Lunelli, B., Maciel Filho, R., Maciel, M. 2014. Simulation of ethanol production via fermentation of the synthesis gas using Aspen Plus TM. *Chem. Eng. Trans.*, 37 (2), 637-642. DOI: 10.3303/CET1437107. Retrieved July 4, 2022, from <https://www.aidic.it/cet/14/37/107.pdf>
- Ashraf, M.T., Schmidt, J.E. 2018. Process simulation and economic assessment of hydrothermal pretreatment and enzymatic hydrolysis of multi-feedstock lignocellulose – Separate vs combined processing. *Bioresour. Technol.* 249, 835–843. DOI: 10.1016/j.biortech.2017.10.088. Retrieved August 12, 2022, from <https://www.sciencedirect.com/science/article/pii/S0960852417319193>
- Bahry, H., Pons, A., Abdallah, R., Pierre, G., Delattre, C., Fayad, N., Taha, S., Vial, C. 2017. Valorization of carob waste: Definition of a second-generation bioethanol production process. *Bioresour. Technol.* 235, 25–34. DOI: 10.1016/j.biortech.2017.03.056. Retrieved August 12, 2022, from <https://www.sciencedirect.com/science/article/pii/S0960852417303267>
- Battista, F., Gomez Almendros, M., Rousset, R., Bouillon, P.-A. 2019. Enzymatic hydrolysis at high lignocellulosic content: Optimization of the mixing system geometry and of a fed-batch strategy to increase glucose concentration. *Renewable Energy* 131, 152–158. Retrieved August 12, 2022, from <https://doi.org/10.1016/j.renene.2018.07.038>
- Borand, M.N., Karaosmanoglu, F. 2018. Effects of organosolv pretreatment conditions for lignocellulosic biomass in biorefinery applications: A review. *J. Renewable Sustainable Energy* 10 (3), 033104. DOI: 10.1063/1.5025876
- Brown, T.R. 2015. A techno-economic review of thermochemical cellulosic biofuel pathways. *Bioresour Technol.* 178 166-176. DOI: 10.1016/j.biortech.2014.09.053. Retrieved May 18, 2022, from <https://pubmed.ncbi.nlm.nih.gov/25266684/>

- Cardona E., Llano B., Peñuela M., Peña J., Rios L.A. 2018. Liquid-hot-water pretreatment of palm-oil residues for ethanol production: an economic approach to the selection of the processing conditions. *Energy*, 160: 441-451. DOI: 10.1016/j.energy.2018.07.045. Retrieved May 18, 2022, from <https://www.sciencedirect.com/science/article/pii/S0360544218313409>
- Chandel, A.K., Garlapati, V.K., Singh, A.K., Antunes, F.A.F., da Silva, S.S. 2018. The path forward for lignocellulose biorefineries: bottlenecks, solutions, and perspective on commercialization. *Bioresour. Technol.* 264, 370–381. DOI: 10.1016/j.biortech.2018.06.004. Retrieved May 18, 2022, from <https://www.sciencedirect.com/science/article/pii/S0960852418307831>
- Chin, D.W.K., Lim, S., Pang, Y.L., Lam, M.K. 2020. Fundamental review of organosolv pretreatment and its challenges in emerging consolidated bioprocessing. *Biofuels, Bioprod. Bioref.* 14 (4), 808–829. DOI: 10.1002/bbb.2096. Retrieved May 18, 2022, from <https://onlinelibrary.wiley.com/doi/abs/10.1002/bbb.2096>
- Choi, J.-H., Jang, S.-K., Kim, J.-H., Park, S.-Y., Kim, J.-C., Jeong, H., Kim, H.-Y., Choi, I.- G. 2019. Simultaneous production of glucose, furfural, and ethanol organosolv lignin for total utilization of high recalcitrant biomass by organosolv pretreatment. *Renewable Energy* 130, 952–960. DOI: 10.1016/j.renene.2018.05.052. Retrieved August 12, 2022, from <https://www.sciencedirect.com/science/article/abs/pii/S0960148118305731>
- Chrysikou, L.P., Bezergianni, S., Kiparissides, C. 2018. Environmental analysis of a lignocellulosic-based biorefinery producing bioethanol and high-added value chemicals. *Sustain. Energy Technol. Assess.* 28, 103–109. DOI: 10.1016/j.seta.2018.06.010. Retrieved August 12, 2022, from <https://www.sciencedirect.com/science/article/abs/pii/S2213138817302679>
- Daylan, B., Ciliz, N. 2016. Life cycle assessment and environmental life cycle costing analysis of lignocellulosic bioethanol as an alternative transportation fuel. *Renew. Energy* 89, 578–587. DOI: 10.1016/j.renene.2015.11.059. Retrieved June 18, 2022, from <https://www.sciencedirect.com/science/article/pii/S0960148115304754>
- Devarapalli, M., Lewis, R.S., Atiyeh, H.K. 2017. Continuous ethanol production from synthesis gas by *Clostridium ragsdalei* in a trickle-bed reactor. *Fermentation* 3 (2), 1-13. DOI: 10.3390/fermentation3020023. Retrieved June 18, 2022, from <https://www.mdpi.com/2311-5637/3/2/23>
- Gabhane M. and Kapoor A., 2019. Simulation of ethanol production process using Aspen plus and optimization based on response surface methodology. *Res. J. Chem. Environ.* 23 (4), 80-89.
- García-Velásquez, Carlos A., Cardona, Carlos A. 2019. Comparison of the biochemical and thermochemical routes for bioenergy production: a techno-economic (TEA), energetic and environmental assessment. *Energy* 172, 232–242. DOI: 10.1016/j.energy.2019.01.073. Retrieved June 18, 2022, from <https://www.sciencedirect.com/science/article/abs/pii/S0360544219300751>
- Gil I.D., Gracia L.C., Rodriguez G. 2014. Simulation of ethanol extractive distillation with mixed glycerol as separating agent. *Braz. J. Chem. Eng.* 31(1): 259-270. DOI: 10.1590/S0104-66322014000100024. Retrieved May 22, 2022, from <https://www.scielo.br/j/bjce/a/CBzxwTCMZnvQmNTt9dGhHwr/>
- Gnansounou, E., Dauriat, A. 2010. Techno-economic analysis of lignocellulosic ethanol: A review. *Bioresour. Technol.* 101 (13), 4980–4991. DOI: 10.1016/j.biortech.2010.02.009. Retrieved July 4, 2022, from <https://www.sciencedirect.com/science/article/abs/pii/S0960852410002804>
- Hoang, P., Ko, J.K., Gong, G., Um, Y., Lee, S.M. 2020. Improved simultaneous co-fermentation of glucose and xylose by *Saccharomyces cerevisiae* for efficient lignocellulosic biorefinery. *Biotechnol. Biofuels* 13 (1). DOI: 10.1186/s13068-019-1641-2. Retrieved June 18, 2022, from <https://biotechnologyforbiofuels.biomedcentral.com/articles/10.1186/s13068-019-1641-2>

- Isikgor, F.H., Becer, C.R. 2015. Lignocellulosic biomass: a sustainable platform for the production of bio-based chemicals and polymers. *Polym. Chem.* 6, 4497–4559. DOI: 10.1039/C5PY00263J Retrieved May 22, 2022, from <https://pubs.rsc.org/en/content/articlelanding/2015/py/c5py00263j>
- Kim, S.M., Dien, B.S., Tumbleson, M., Rausch, K.D., Singh, V. 2016. Improvement of sugar yields from corn stover using sequential hot water pretreatment and disk milling. *Bioresour. Technol.* 216, 706–713. DOI: 10.1016/j.biortech.2016.06.003. Retrieved May 22, 2022, from <https://www.sciencedirect.com/science/article/pii/S096085241630801X>
- Kim, S.M., Tumbleson, M., Rausch, K.D., Singh, V. 2017. Impact of disk milling on corn stover pretreated at commercial scale. *Bioresour. Technol.* 232, 297–303. DOI: 10.1016/j.biortech.2017.02.005 Retrieved July 4, 2022, from <https://www.sciencedirect.com/science/article/abs/pii/S0960852417301104>
- Kumar, D., Singh, V. 2016. Dry-grind processing using amylase corn and superior yeast to reduce the exogenous enzyme requirements in bioethanol production. *Biotechnol. Biofuels* 9, 228. DOI: 10.1186/s13068-016-0648-1. Retrieved June 18, 2022, from <https://biotechnologyforbiofuels.biomedcentral.com/articles/10.1186/s13068-016-0648-1>
- Li K., Qin J.C., Liu C.G., Bai F.W. 2016. Optimization of pretreatment, enzymatic hydrolysis, and fermentation for more efficient ethanol production by jerusalem artichoke stalk. *Bioresour. Technol.*, 221: 188–194. DOI: 10.1016/j.biortech.2016.09.021. Retrieved July 4, 2022, from <https://www.sciencedirect.com/science/article/pii/S0960852416312767>
- Morales M., Arvesen A., Cherubini F. 2021. Integrated process simulation for bioethanol production: Effects of varying lignocellulosic feedstocks on technical performance. *Bioresource Technology* 328:124833. DOI: 10.1016/j.biortech.2021.124833. Retrieved May 16, 2022, from <https://www.sciencedirect.com/science/article/pii/S0960852421001723>
- Morales, M., Quintero, J., Aroca, G. 2017. Environmental assessment of the production and addition of bioethanol produced from *Eucalyptus globulus* to gasoline in Chile. *Int. J. Life Cycle Assess.* 22 (4), 525–536. DOI: 10.1007/s11367-016-1119-4. Retrieved July 4, 2022, from <https://link.springer.com/article/10.1007/s11367-016-1119-4>
- Nosrati-Ghods N., Naidoo M., Harrison S.T.L., Isafiade A.J., Tai S.L. 2020. Embedding Aspen Custom Modeller for Bioethanol Fermentation Into the Aspen Plus Flowsheet Simulator. *Chem. Eng. Transactions* 80, 289–294. DOI: 10.3303/CET2080049. Retrieved July 4, 2022, from <https://www.cetjournal.it/index.php/cet/article/view/CET2080049>
- Oliva, J.M., Negro, M.J., Alvarez, C., Manzanares, P., Moreno, A.D. 2020. Fermentation strategies for the efficient use of olive tree pruning biomass from a flexible biorefinery approach. *Fuel* 277, 118171. DOI: 10.1016/j.fuel.2020.118171. Retrieved May 16, 2022, from <https://www.sciencedirect.com/science/article/abs/pii/S0016236120311674>
- Olofsson J., Barta Z., Börjesson P. and Wallberg O. 2017. Integrating enzyme fermentation in lignocellulosic ethanol production: lifecycle assessment and techno-economic analysis. *Biotechnol Biofuels* 10(1), 51. DOI: 10.1186/s13068-017-0733-0. Retrieved May 16, 2022, from <https://biotechnologyforbiofuels.biomedcentral.com/articles/10.1186/s13068-017-0733-0>
- Rodrigues G., Errico, M., Rong, B.G. 2018. Techno-economic analysis of organosolv pretreatment process from lignocellulosic biomass. *Clean Technol. Environ. Policy* 20, 1401–1412. DOI: 10.1007/s10098-017-1389-y. Retrieved May 16, 2022, from <https://link.springer.com/article/10.1007/s10098-017-1389-y>
- Romaní, A., Larramendi, A., Yáñez, R., Cancela, A., Sánchez, A., Teixeira, J.A., Domínguez, L. 2019. Valorization of *Eucalyptus nitens* bark by organosolv pretreatment for the production of advanced biofuels. *Ind. Crops Prod.* 132, 327–335. DOI: 10.1016/j.indcrop.2019.02.040. Retrieved May 16, 2022, from <https://www.sciencedirect.com/science/article/abs/pii/S0926669019301414>

Sarks, C., Jin, M., Sato, T.K., Balan, V., Dale, B.E. 2014. Studying the rapid bioconversion of lignocellulosic sugars into ethanol using high cell density fermentations with cell recycle. *Biotechnol. Biofuels* 7 (1), 73. DOI: 10.1186/1754-6834-7-73. Retrieved May 16, 2022, from <https://biotechnologyforbiofuels.biomedcentral.com/articles/10.1186/1754-6834-7-73>

Sharma, B., Larroche, C., Dussap, C.-G. 2020. Comprehensive assessment of 2G bioethanol production. *Bioresour. Technol.* 313, 123630. DOI: 10.1016/j.biortech.2020.123630. Retrieved June 20, 2022, from <https://www.sciencedirect.com/science/article/abs/pii/S0960852420309020>

Singh, A. and Rangaiah, G.P. 2017. Review of technological advances in bioethanol recovery and dehydration. *Ind. Eng. Chem. Res.* 56 (18): 5147-5163. DOI: 10.1021/acs.iecr.7b00273. Retrieved June 20, 2022, from <https://pubs.acs.org/doi/10.1021/acs.iecr.7b00273>

Tan, L.i., Zhong, J., Jin, Y.-L., Sun, Z.-Y., Tang, Y.-Q., Kida, K. 2020. Production of bioethanol from unwashed-pretreated rapeseed straw at high solid loading. *Bioresour. Technol.* 303, 122949. DOI: 10.1016/j.biortech.2020.122949. Retrieved June 20, 2022, from <https://www.sciencedirect.com/science/article/abs/pii/S0960852420302182>

Vieira, S., Barros, M.V., Sydney, A.C.N., Piekarski, C.M., de Francisco, A.C., Vandenberghe, L.P.D.S., Sydney, E.B. 2020. Sustainability of sugarcane lignocellulosic biomass pretreatment for the production of bioethanol. *Bioresour. Technol.* 299, 122635. Retrieved June 20, 2022, from <https://www.sciencedirect.com/science/article/pii/S0960852419318656>

Zabed, H., Sahu, J., Suely, A., Boyce, A., Faruq, G. 2017. Bioethanol production from renewable sources: current perspectives and technological progress. *Renew. Sust. Energ. Rev.* 71, 475–501. DOI: 10.1016/j.rser.2016.12.076. Retrieved May 18, 2022, from <https://www.sciencedirect.com/science/article/abs/pii/S1364032116311339>

Zabed, H., Sahu, J.N., Boyce, A.N. and Faruq, G. 2016. Fuel ethanol production from lignocellulosic biomass: An overview on feedstocks and technological approaches. *Renewable Sustainable Energy Rev.* 66, 751-774. DOI: 10.1016/j.rser.2016.08.038. Retrieved May 18, 2022, from <https://www.sciencedirect.com/science/article/abs/pii/S1364032116304695>

Zhang, K.e., Pei, Z., Wang, D. 2016. Organic solvent pretreatment of lignocellulosic biomass for biofuels and biochemicals: A review. *Bioresour. Technol.* 199, 21–33. DOI: 10.1016/j.biortech.2015.08.102 Retrieved May 18, 2022, from <https://www.sciencedirect.com/science/article/pii/S0960852415012080>

Zhou, Z., Lei, F., Li, P., Jiang, J. 2018. Lignocellulosic biomass to biofuels and biochemicals: A comprehensive review with a focus on ethanol organosolv pretreatment technology. *Biotechnol. Bioeng.* 115 (11), 2683–2702. DOI: 10.1002/bit.26788. Retrieved May 18, 2022, from <https://onlinelibrary.wiley.com/doi/abs/10.1002/bit.26788>